Int J Thermophys (2010) 31:888–899
DOI 10.1007/s10765-009-0700-5

Feasibility Study of a Novel Technique for Measurement of Liquid Thermal Conductivity with a Micro-beam Sensor

Hiroshi Takamatsu · Kyosuke Inada · Satoru Uchida · Koji Takahashi · Motoo Fujii

Received: 12 June 2009 / Accepted: 31 December 2009 / Published online: 22 January 2010

Abstract A new method was proposed to measure the thermal conductivity of liquids with infinitesimal samples, which are much smaller than those required in conventional methods. The method utilizes a micro-beam-type MEMS sensor fabricated across a trench on a silicon substrate. Numerical analysis of heat conduction within and around a uniformly heated sensor showed that the temperature of a 10 μm long sensor reached a steady state within approximately 0.1 ms, after the start of heating. It was also revealed that the average temperature of the sensor at the steady state was higher in liquids with lower thermal conductivity. These results demonstrate a new idea of measuring the thermal conductivity of liquids within an extremely short time at a steady state before the onset of natural convection.

Keywords Measurement technique · MEMS sensor · Numerical analysis · Thermal conductivity

1 Introduction

The transient hot-wire method has been developed as the most reliable and popular method to measure the thermal conductivity of gases and liquids [1–5]. These hot-wire

H. Takamatsu (✉) · K. Inada · S. Uchida
Department of Mechanical Engineering, Kyushu University, 744 Motooka, Fukuoka 819-0395, Japan
e-mail: takamatsu@mech.kyushu-u.ac.jp

K. Takahashi
Department of Aeronautics and Astronauts, Kyushu University, 744 Motooka, Fukuoka 819-0395, Japan

M. Fujii
National Institute of Advanced Industrial Science and Technology, 744 Motooka, Fukuoka 819-0395, Japan

instruments were designed so that the measured temperature increase in the wire could be compared with an analytical solution to a radial heat conduction equation. Thin and long wires, about 10 μm in diameter and several hundred millimeters long, were used to eliminate the effect of the axial temperature distribution in the wire. In addition, two cells with respective wires of different lengths were employed to compensate the end effects [4,5]. In contrast, Fujii and co-workers have developed a short-hot-wire method [6–8], which assumed a heat loss from both ends of a wire to the power terminals. The theoretical increase in the wire temperature was obtained from a numerical solution to a two-dimensional heat conduction equation. One of the advantages of the short-hot-wire method is that it requires smaller samples than the transient hot-wire method; it requires only several tens of milliliters while the latter generally needs more than 100 ml.

Much less volume is required in a forced Rayleigh scattering method [9,10], which utilizes irradiation of pulsed high-power laser beams on the sample surface. This method has another advantages resulting from its contact-free measurement and extremely short time for measurement. However, it measures only the thermal diffusivity of liquids.

The goal of our study is to develop a method for measuring the thermal conductivity of fluids with a small volume, 1 μL, for instance, as a target. The method may be useful for samples that are available only in small quantities, such as those being synthesized on a research basis, biological fluids, and other valuable liquids. We designed a micro-sensor fabricated on a silicon chip. Although the basic idea of the sensor is similar to that of the short-hot-wire method, a significant difference in size could result in a considerable difference in the transient temperature rise. An expected, a quick increase in the temperature with a micro-sensor might place restrictions on the size of the sensor for measurements within an acceptable uncertainty due to the limited time response of measuring instruments. In addition, a theoretical temperature increase should be obtained by a three-dimensional analysis for heat conduction because symmetric geometry cannot be fabricated by silicon technologies. The objective of this preliminary study was therefore to examine the feasibility of the measurement of thermal transport properties using a MEMS sensor. Based on a numerical analysis for heat conduction within the sensor and its surroundings, we propose a new method for measuring the thermal conductivity of liquids.

2 Micro-beam Sensor

Figure 1 shows the design of a "micro-beam sensor" that we propose in the present work. A thin platinum beam-type sensor is to be fabricated on a substrate to form a bridge across a trench by etching a platinum film deposited on a silicon substrate. The typical thickness of the sensor will be scores of nanometers, and its length will be several micrometers. The sensor is intended to be submerged in a small liquid pool that is made on the substrate (not shown in Fig. 1). The temperature of the sensor is recorded after stepwise heating of the sensor by applying a direct electric current.

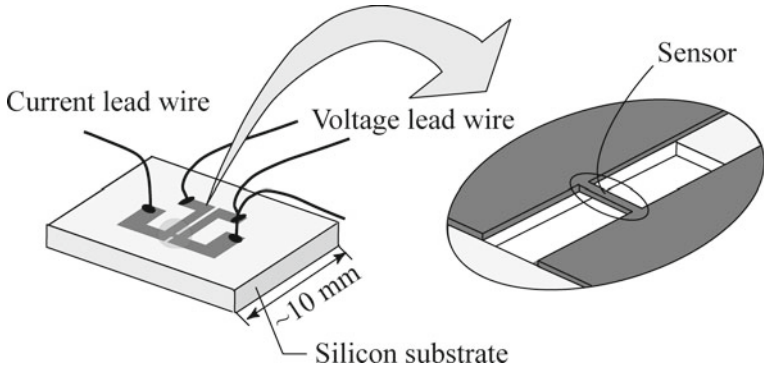

Fig. 1 Schematic of the micro-beam sensor fabricated on a silicon chip

3 Transient Heat Conduction Analysis

3.1 Physical Model

Figure 2 shows the physical model of the sensor shown in Fig. 1. A rectangular beam sensor of width $2a$, thickness $2b$, and length $2l$ is heated uniformly in a liquid sample. The temperature at the sensor–substrate interface is assumed to remain constant at the initial temperature due to the large heat capacity of the substrate. Transient heat conduction equations in the sensor and the surrounding liquid are described in dimensionless forms:

$$\frac{\partial \Theta_s}{\partial Fo} = \left(\frac{\partial^2 \Theta_s}{\partial X^2} + \frac{\partial^2 \Theta_s}{\partial Y^2} + \frac{\partial^2 \Theta_s}{\partial Z^2} \right) + 1 \tag{1}$$

$$\frac{\partial \Theta_f}{\partial Fo} = A \left(\frac{\partial^2 \Theta_f}{\partial X^2} + \frac{\partial^2 \Theta_f}{\partial Y^2} + \frac{\partial^2 \Theta_f}{\partial Z^2} \right) \tag{2}$$

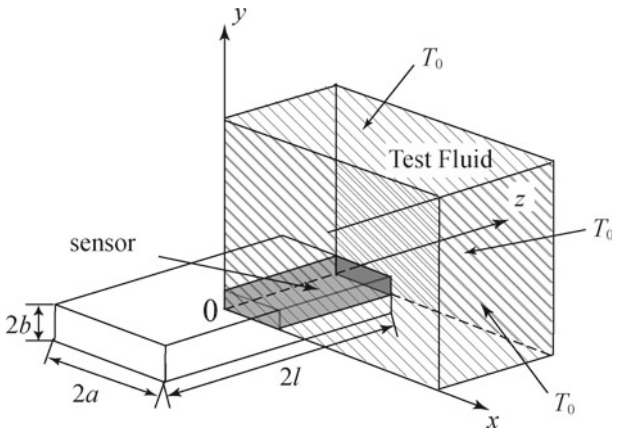

Fig. 2 Physical model of the sensor suspended in a liquid for heat conduction analysis

The initial condition and boundary conditions are

$$\Theta_s = \Theta_f = 0 \quad \text{at } Fo = 0 \tag{3}$$

and

$$\frac{\partial \Theta_s}{\partial X} = \frac{\partial \Theta_f}{\partial X} = 0 \quad \text{at } X = 0 \tag{4}$$

$$\frac{\partial \Theta_s}{\partial Y} = \frac{\partial \Theta_f}{\partial Y} = 0 \quad \text{at } Y = 0 \tag{5}$$

$$\frac{\partial \Theta_s}{\partial Z} = \frac{\partial \Theta_f}{\partial Z} = 0 \quad \text{at } Z = 0 \tag{6}$$

$$\Theta_s = \Theta_f = 0 \quad \text{at } Z = L \tag{7}$$

$$\Theta_f = 0 \quad \text{at } X, Y \to \infty \tag{8}$$

$$\frac{\partial \Theta_s}{\partial X} = \Lambda \frac{\partial \Theta_f}{\partial X} \quad \text{at } X = W \tag{9}$$

$$\frac{\partial \Theta_s}{\partial Y} = \Lambda \frac{\partial \Theta_f}{\partial Y} \quad \text{at } Y = 1 \tag{10}$$

Non-dimensional variables are defined as

$$\Theta = (T - T_0) \Big/ \frac{\dot{q}_v b^2}{\lambda_s}, \quad Fo = \frac{\alpha_s t}{b^2}, \quad A = \frac{\alpha_f}{\alpha_s}, \quad \Lambda = \frac{\lambda_f}{\lambda_s}, \quad X = \frac{x}{b},$$
$$Y = \frac{y}{b}, \quad Z = \frac{z}{b}, \quad L = \frac{l}{b}, \quad W = \frac{a}{b}$$

where T is the temperature (K), $\dot{q}_v$ is the heat generation ($W \cdot m^{-3}$), λ is the thermal conductivity ($W \cdot m^{-1} \cdot K^{-1}$), α is the thermal diffusivity ($m^2 \cdot s^{-1}$), and t is the time (s). The subscripts s and f stand for the sensor and the fluid, respectively. We solved these equations for two sensors that have different lengths, $L = 100$ and 200, but have the same width $W = 10$. Taking into account the symmetric geometry, the solution domain was defined by one-eighth of the whole region, which is shown as a rectangular block with hatched lines in Fig. 2. The size of the domain in X- and Y-dimensions was 300 for the sensor of $L = 100$ and 500 for that of $L = 200$. We used Eq. 7 as a boundary condition in the present feasibility study, although a domain larger than L in the Z-dimension should be defined in the fluid region in the strict sense. A platinum sensor and water as the test fluid were chosen for the preliminary calculation. Given parameters were $\Lambda = 0.0129$ and $A = 0.00862$, which were obtained with properties of platinum film [11]: $\lambda_s = 47.25\,W \cdot m^{-1} \cdot K^{-1}$ and $\alpha_s = 1.69 \times 10^{-5}\,m^2 \cdot s^{-1}$. Numerical solutions were obtained by the finite element method using MSC Marc/Mentat software on the computing system for research in Kyushu University. The solution domain was divided into rectangular elements with the size $1.0(X) \times 1.0(Y) \times 2.5(Z)$ in the sensor and $0.5(X) \times 0.5(Y) \times 2.5(Z)$ in the vicinity of the sensor. The size in X- and Y-dimensions was increased at $X \geq 15$ and $Y \geq 15$. The total number of elements was 91430 for $L = 100$ and 210880 for $L = 200$. The error in the heat balance at the sensor was smaller than 2 %.

3.2 Results

Figure 3 shows a change in the temperature distribution in the sensor at the center of the cross section along the *Z*-axis ($X = Y = 0$), and Fig. 4 shows that in the fluid along the *Y*-axis ($X = Z = 0$) from the midpoint of the sensor. The temperature in the sensor approached an arched distribution because the sensor-substrate interface was kept at the initial temperature. The temperature in the liquid increased with increasing temperature at the sensor, resulting in the expansion of a thermally affected region in the liquid. Both figures show that only a small difference was found in the temperature distribution between $Fo = 0.5 \times 10^6$ and $Fo = 4.0 \times 10^6$.

Figure 5 shows the transient temperature rise in the sensor as a function of *Fo*. The average temperature as well as the temperature at the center increased abruptly after the start of heating but stopped increasing at a certain temperature. This is not the case

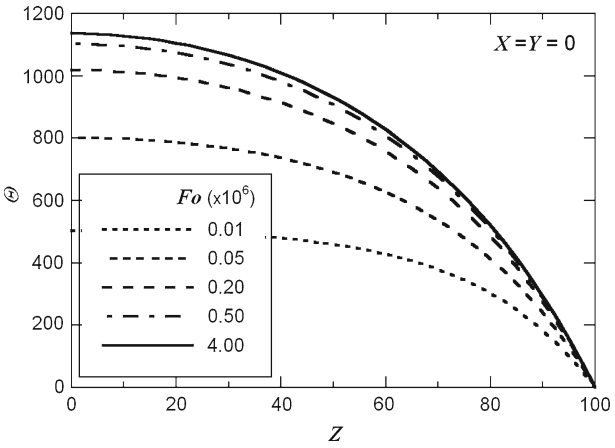

Fig. 3 Distribution of dimensionless temperature in the sensor along *Z*-axis

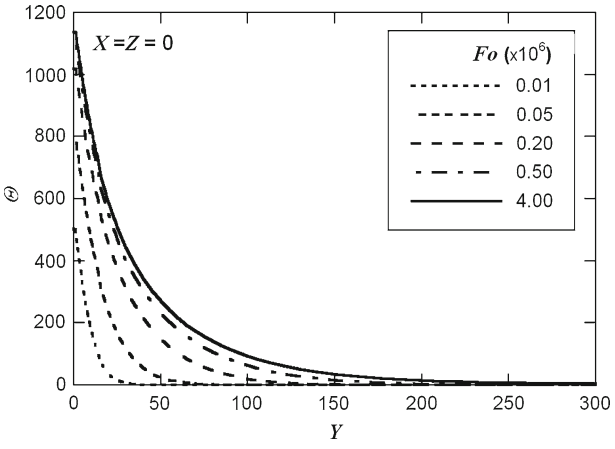

Fig. 4 Distribution of dimensionless temperature in the liquid along *Y*-axis

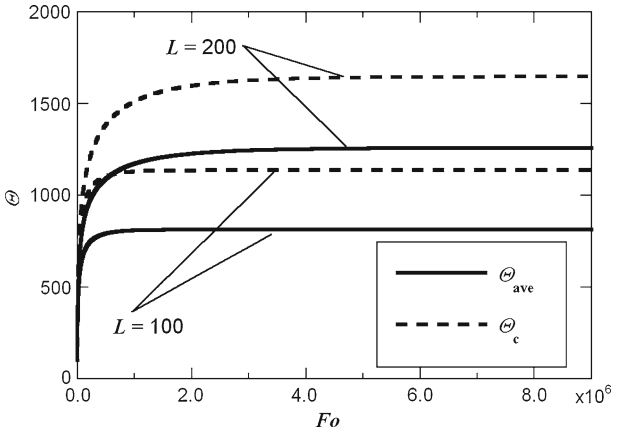

Fig. 5 Change in the dimensionless temperature increase in the sensor

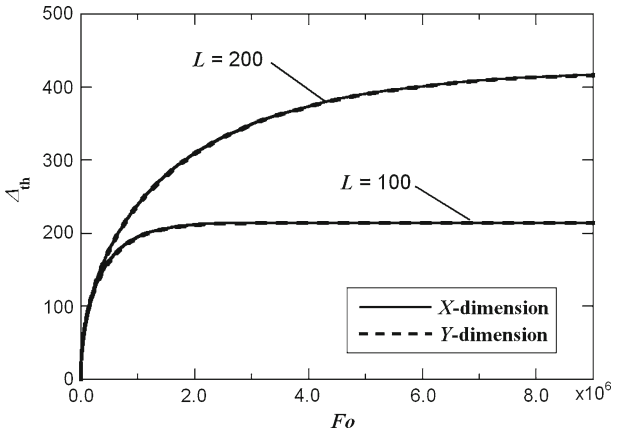

Fig. 6 Change in the dimensionless thickness of thermally affected region in the liquid

in the solution to the one-dimensional radial heat conduction equation, which is used in the transient hot-wire method; the temperature of an infinitely long wire continues to increase during heating. The difference results from the boundary condition that the temperature remains unchanged at both ends. The final temperature was lower at the shorter sensor, since only the temperature at the middle part of the sensor increased to become an arched distribution as shown in Fig. 3. The time required to reach the steady state was also shorter for a shorter sensor.

The thickness of the thermally affected region also increased towards a constant value as shown in Fig. 6, where the thickness Δ_{th} was defined by the distance from the center to the point on the X- or Y-axis where the temperature rise was 1 % of that at the center. While the width of the sensor was 10 times larger than the thickness, $X_{\mathrm{s}} = 10$, the values of Δ_{th} in the X- and Y-dimensions were almost the same as shown in Fig. 6. The time required to reach the steady state was longer for Δ_{th} than the average temperature of the sensor, suggesting that the temperature in the sensor was not as sensitive to Δ_{th} after the temperature distribution has been almost developed.

Here, we assume the thickness of the sensor to be 50 nm, taking into account the fabrication process. The time during which the average temperature of the sensor increased up to 99 % of the final temperature rise was $Fo \approx 7.9 \times 10^5$ for the sensor of $L = 100$ and $Fo \approx 3.2 \times 10^6$ for that of $L = 200$. This indicates that the average temperature of the sensor reaches almost a steady state at 29 μs after heating a 5 μm long sensor and 116 μs for a sensor of 10 μm length. The measurement of the transient temperature response, which is necessary in the transient hot-wire method, therefore requires extremely high time resolution in the measurement instruments, and might be difficult in practice. However, the results suggest that the steady-state temperature field that is governed only by heat conduction may be established before natural convection takes place around a sensor. Therefore, we will next examine the feasibility of measuring the thermal conductivity at the steady state instead of measurements of the transient temperature response.

4 Steady-State Heat Conduction Analysis for Measuring Thermal Conductivity

4.1 Physical Model

The physical model shown in Fig. 2 was used again for the steady-state analysis. Equations 1 and 2 were solved with substituting zero for the left-hand side using the boundary conditions described by Eqs. 4– 10. The solution domain and the grids used were the same as those for the transient conduction analysis.

4.2 Temperature in the Sensor for Given Thermal Conductivity of Liquids

Figure 7 shows the dimensionless average temperature Θ_{ave} in the sensor as a function of the dimensionless thermal conductivity Λ of liquids. The range $\Lambda = 0.001$ to 0.2 given in the analysis covers all possible thermal conductivities of liquids at atmospheric pressure and room temperature. Typical values are: 0.0012 for FC-72, 0.0028 for toluene, 0.013 for water, and 0.17 for mercury, for instance. The value of Θ_{ave} is higher for smaller Λ as expected. It is significant except for Λ larger than 0.02 where the temperature rise is negligibly small. This indicates that the thermal conductivity of liquids, excluding liquid metals, could be determined by measuring the average temperature rise in the sensor, $T_{\text{ave}} - T_0$. Dependence of Θ_{ave} on Λ is larger for a longer sensor; Θ_{ave} at $\Lambda = 0.001$ as compared with that at $\Lambda = 0.01$ is 4.8 fold for a sensor of $L = 200$ and 2.7 fold for that of $L = 100$. This is because the heat loss from the sensor to the substrate is larger in a shorter sensor as will be shown in Fig. 9 in the next section. The result suggests that a longer sensor has an advantage for the measurement.

4.3 Examination for Measurement

The thickness of the thermally affected region Δ_{th} was independent of the thermal conductivity of liquids. It increased in proportion to the length of the sensor as shown

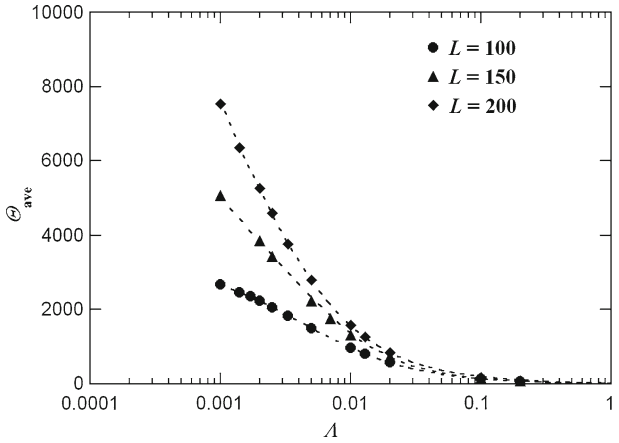

Fig. 7 Dimensionless average temperature rise in the sensor as a function of the dimensionless thermal conductivity of liquids

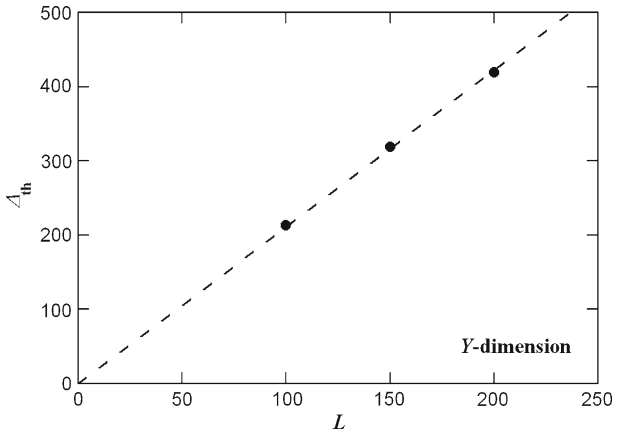

Fig. 8 Effect of the sensor length on the dimensionless thickness of thermally affected region in the liquid

in Fig. 8. The temperature of the liquid increased around the sensor within a distance that is nearly the same as the length of the sensor, $2l$. Therefore we need to prepare more than a 5 μm deep trench beneath a 5 μm long sensor.

Figure 9 shows the heat loss from the sensor to the substrate compared with the generated heat as a function of Λ. The heat loss is larger in shorter sensors and liquids with smaller thermal conductivity. Since the percent heat loss was 83 % in the sensor of $L = 100$ in the liquid of $\Lambda = 0.001$, a longer sensor should be employed for the liquid with such a low thermal conductivity.

Figure 10 shows the average temperature rise in the sensor as a function of the electric current squared, I^2, for water, toluene, and FC-72. The temperature rise increases in proportion to I^2 because $T - T_0$ $(= \dot{q}_v b^2/\lambda_s \Theta)$ is in proportion to the heat generation per unit volume, $\dot{q}_v$, which is given by

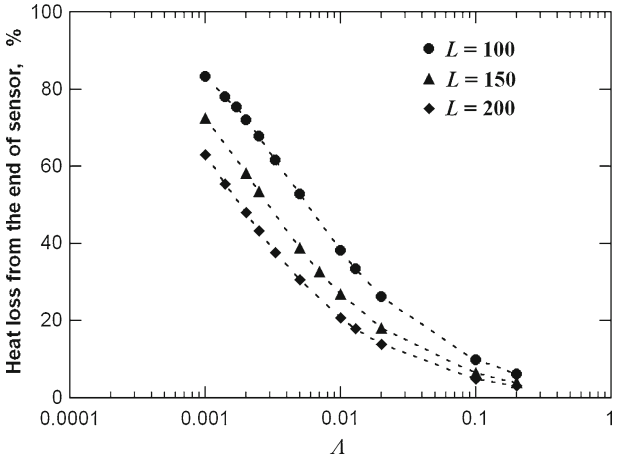

Fig. 9 Effect of the liquid thermal conductivity on the percent heat loss from the sensor to the substrate

$$\dot{q}_{\mathrm{v}} = \frac{I^2 R}{abl} \tag{11}$$

The temperature rise for FC-72 is 5.8 times larger than that for water for which the thermal conductivity is 10.8 times as large as that of FC-72. The electric resistance R of the sensor is approximately 170 Ω in a sensor, 50 nm × 0.5 μm × 10 μm in size, which was estimated from the electrical resistivity of 0.42 μΩ · m [11]. If we assume that a temperature rise of 3 K is required for the measurement, the applied current should be 0.23 mA in water and 0.09 mA in FC-72, which yields 39 mV and 15 mV, respectively, in the voltage drop in the sensor. We are able to measure and control these magnitudes of the current and the voltage by using ordinary instruments.

The thermal conductivity of test liquids is derived from the measurement of the temperature rise $T_{\mathrm{ave}} - T_0$ using the relation in Fig. 7 expressed as

$$\Lambda = f\left(\Theta_{\mathrm{ave}}\right) \tag{12}$$

Differentiation of Eq. 12 with the definition of Λ and Θ allows us to estimate the uncertainty in the measured thermal conductivity from

$$\frac{\delta\lambda_{\mathrm{f}}}{\lambda_{\mathrm{f}}} = \left[\left(\frac{f'}{f}\Theta_{\mathrm{ave}}\right)^2\left\{\left(\frac{\delta\left(T_{\mathrm{ave}} - T_0\right)}{T_{\mathrm{ave}} - T_0}\right)^2 + \left(\frac{\delta\dot{q}_{\mathrm{v}}}{\dot{q}_{\mathrm{v}}}\right)^2 + \left(2\frac{\delta b}{b}\right)^2\right\} + \left(\frac{f'}{f}\Theta_{\mathrm{ave}} + 1\right)^2\left(\frac{\delta\lambda_{\mathrm{s}}}{\lambda_{\mathrm{s}}}\right)^2\right]^{1/2} \tag{13}$$

where f' is the derivative of f by Θ_{ave} which is calculated from Eq. 12. The estimated uncertainty was 9.7 % for water, 10.9 % for toluene, and 13.1 % for FC-72. These were evaluated with the temperature coefficient of platinum film [11] and the

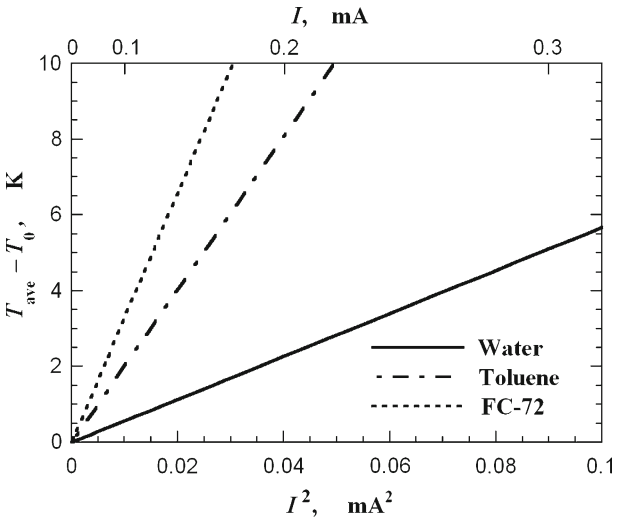

Fig. 10 Average temperature rise in the sensor as a function of applied current squared

hypothesized accuracy of measurement in the voltage and sizes. The uncertainty in the thermal conductivity of the platinum sensor was also assumed to be 5 %. This is the main source of the uncertainty of the thermal conductivity but may be reduced in practical measurements. In general, prior to the measurement with test fluids, the electrical and thermal properties of the sensor will be obtained in a vacuum chamber and some standard liquids with known thermal conductivities. With these calibrations we are able to eliminate the uncertainty in the thermal conductivity of the sensor, and reduce the uncertainty to 2.5 % for water, 3.2 % for toluene, and 4.4 % for FC-72.

It is inevitable that the estimated uncertainty in the present method is larger than that in the transient hot-wire method or the short-hot-wire method. However, the proposed sensor can be used in a variety of applications. One of the merits of the MEMS sensor is that multiple sensors with similar properties are fabricated easily. Even if they have some deviations in the properties, we can determine them by using an apparatus that is specialized for calibration if the sensor and terminals are mounted on a single chip. This is not the case in the transient hot-wire method and the short-hot-wire method where a thin wire is spot-welded to terminals that are mounted on the experimental setup. The utilization of MEMS sensors might therefore allow us to develop the first instrument on the market to measure the thermal conductivity of liquids. The sensor may be also used in instruments such as chromatographs or for the purpose of quality control of products in industrial processes via measurements of the thermal conductivity.

5 Conclusions

We have proposed a MEMS sensor to demonstrate that the sensor is useful for measuring the thermal conductivity of liquids by a new method. A “micro-beam sensor”

was proposed to be fabricated across a trench created on a silicon substrate. We found by numerical analysis of transient heat conduction in the sensor and the surrounding liquid that the temperature in the sensor approached a steady state quickly after the start of heating. For instance, a sensor 50 nm thick and 10 μm long reaches a steady state within approximately 100 μs. The numerical analysis also confirmed that the average temperature at the steady state depended significantly on the thermal conductivity of the surrounding liquid. The unique feature of the temperature rise of the proposed micro-beam sensor allows us to develop a technique for deriving the thermal conductivity of liquids from the measurement of the temperature at the steady state. Results from the present work also gave some important criteria for fabrication of the sensor. The depth of the trench should be longer than the length of the sensor if a thermally affected region is not allowed to reach the bottom. The length of the sensor should be determined from the range of thermal conductivity to be measured by taking into account the percent heat loss from the sensor–substrate interface. The uncertainty of the thermal conductivity measured by the proposed method with a 50 nm × 0.5 μm × 10 μm sensor was estimated to be 2.5 % for water, 3.2 % for toluene, and 4.4 % for FC-72.

The next step of our study will be to demonstrate the measurement of the thermal conductivity of small liquid samples by using the micro-beam sensor, which was proposed only by numerical simulation in the present work. We do know that the beam sensor that has an ideal rectangular shape, which we assumed in the present paper, is difficult to fabricate. The top view of the sensor may become the shape of the letter "I" because the substrate near the root of the sensor is also eroded by the wet etching process. It is also difficult to make a deep trench under the sensor. However, once a sensor is fabricated and observed by using a scanning electron microscope, for instance, numerical analysis can be performed for the system for the given configurations and dimensions. The principle and fundamental knowledge obtained in the present study will work for a practical sensor that has a shape more or less different from the present study.

We also have some other problems to overcome. At this moment, we have no idea about the strength of such a small sensor. Electrical insulation will be needed for measuring conductive liquids. There might be some other problems that are unique to MEMS sensors. Although the problems to be solved remain, we believe that the present work is valuable in that it exhibited a new way to measure the thermal conductivity of liquids.

Acknowledgment This work was supported by a Grant-in-Aid for Scientific Research from the Japan Society for the Promotion of Science (No. 20656039).

References

1. M.J. Assael, C.A. Nieto de Castro, H.M. Roder, W.A. Wakeham, in *Measurement of the Transport Properties of Fluids, Experimental Thermodynamics*, vol. III, ed. by W.A. Wakeham, A. Nagashima, J.V. Senger (Blackwell Scientific Publications, Oxford, 1991), p. 163
2. J. Kestin, R. Paul, A.A. Clifford, W.A. Wakeham, Physica A **100**, 349 (1980)
3. Y. Nagasaka, A. Nagashima, Rev. Sci. Instrum. **52**, 229 (1981)

4. G.C. Maitland, M. Mustafa, M. Ross, R.D. Trengov, W.A. Wakeham, M. Zalaf, Int. J. Thermophys. **7**, 245 (1986)
5. K. Kawamata, Y. Nagasaka, A Nagshima, Int. J. Thermophys. **9**, 317 (1988)
6. M. Fujii, X. Zhang, N. Imaishi, S. Fujiwara, T. Sakamoto, Int. J. Thermophys. **18**, 327 (1997)
7. X Zhang, M. Fujii, Int. J. Thermophys. **21**, 71 (2000)
8. H. Xie, H. Gu, M. Fujii, X. Zhang, Meas. Sci. Technol. **17**, 208 (2006)
9. Y. Nagasaka, T. Hatakeyama, M. Okuda, A. Nagashima, Rev. Sci. Instrum. **59**, 1156 (1988)
10. M. Motosuke, Y. Nagasaka, A. Nagashima, Int. J. Thermophys. **25**, 519 (2004)
11. Q.G. Zhang, B.Y. Cao, X. Zhang, M. Fujii, K. Takahashi, J. Phys. Condens. Matter **18**, 7937 (2006)